ARMA 10- 336

Limits of Applicability of the Finite Element Explicit Joint Model in the Analysis of Jointed Rock Problems

Riahi, A. and Hammah, E.R.
Rocscience Inc., Toronto, Canada
780-439 University Avenue, Toronto, Ontario M5G 1Y8

Curran, J.H.
R.M. Smith Professor Emeritus
Civil Engineering Department, University of Toronto,
Toronto, Ontario M5S 1A4
and Rocscience Inc.

ABSTRACT: This paper compares the governing equations and kinematics of joint elements used in continuum numerical methods to those of contact enforcement methods used in discrete element techniques. It provides guidelines for choosing between discontinuous techniques (namely, the distinct element method and the discontinuous deformation analysis) and continuum techniques (such as the finite element method) with joint elements in the analysis of problems with pre-existing discrete fractures.

1. INTRODUCTION

Discontinuities, such as fractures and joints, are surfaces that represent a jump in the displacement field as well as stress and strain fields. The presence of these surfaces reduces the elastic and strength properties of materials, and introduces directional preference, i.e., anisotropy, in material response. When prevalent, discontinuities form a microstructure or fabric and introduce scale effects (behavior governed by the size of discrete bodies relative to the overall scale of a problem).

Three approaches are commonly used to model the discontinuous behavior of jointed rock masses. These are

1. Cosserat continuum methods,
2. Combined continuum-interface methods, which are continuum methods with special joint/interface elements that model discontinuous behavior, and
3. Discrete element techniques.

This paper compares the formulation of combined continuum-interface numerical methods to that of discrete techniques, when both are applied to jointed rock problems. It intends to show the similarities and differences between these formulations, and to provide guidelines on how to choose between discontinuous techniques (namely, the distinct element method [1-4], discontinuous deformation analysis [5]) and combined continuum-interface methods in jointed rock analysis.

The governing equations and kinematics of both joint elements and contact enforcement are discussed. An example of an edge-to-edge contact is solved in closed-form using both techniques.

By comparing results of these methods to closed-form solutions, and discussing the kinematic assumptions of the techniques, the paper concludes that the mathematical terms of FEM interface elements are equivalent to those of contacts in the discrete element models. For a specified input geometry and set of assumptions on the deformability of intact material, combined continuum-interface methods and discrete techniques yield similar results, provided contacts between elements remain unchanged throughout the solution process. If the contacts change, then discrete element techniques provide more realistic results.

For practical geotechnical modeling, the FE-interface model is more desirable because of its ability to quickly analyze several models with varying network geometries and material properties. This feature allows engineers to explore the effects of parameter uncertainty on potential mechanisms, and to develop more robust slope designs and stability measures.

2. GOVERNING EQUATIONS

2.1. Governing equations of solid continua

In continuum solid mechanics, the motion and deformation of a characteristic volume of material – an infinitesimal, homogeneous volume free of gaps, discontinuities, fractures, or inclusions – is described by the linear and angular momentum equations.

The linear momentum equation is expressed as

$$\frac{\partial u_j}{\partial t^2}\rho + \sigma_{ij,i} + b_j = 0\,,^{1} \tag{1}$$

where $\mathbf{u}$ is the displacement, $\boldsymbol{\sigma}$, the Cauchy stress tensor, $\mathbf{b}$, the body force, and ρ, the density of material, respectively.

In the absence of inertial and damping terms, Equation (1) reduces to the static equilibrium expression

$$\sigma_{ij,i} + b_j = 0\,. \tag{2}$$

In the classical theory of elasticity, conservation of angular momentum for the characteristic volume requires symmetry of the Cauchy stress tensor and minor symmetry of the elasticity tensor. Thus angular momentum is implicitly satisfied at each material point when the components of the Cauchy stress tensor are reduced to 6.

There are two equivalent forms of expressing the linear momentum equation. The first form, which comprises Equation (1) and traction boundary conditions, is called the strong form. The second form, known as the weak or variational form, is derived through application of the principle of virtual work. Some numerical techniques, such as the Finite Difference Method (FDM), directly discretize and solve the strong form of the governing equations, while others such as the Finite Element Method (FEM) discretize and solve the weak form.

In the analysis of discrete problems three aspects need to be recognized. These are

(i) Simulation of the deformability of a block, i.e., the $\sigma_{ij,i}$ term in Equation (1), requires a continuum method such as the FEM, FDM, or boundary element method (BEM) [6-9].

(ii) Continuum methods have the ability to accommodate both small and large deformations.

(iii) To relax the assumption of continuity intrinsic to the governing equations for a characteristic volume, continuum methods need special formulations.

[1] Throughout this paper, bold fonts refer to vector or matrix quantities, while components of these quantities are described with non-bolded, italicized fonts with sub-indices.

In continuum-based methods, two main approaches are used to reflect discontinuous material behavior: (1) interface or joint elements [10-15], and (2) micropolar or Cosserat theory [16-19]. This paper focuses on the explicit simulation of interfaces through joint elements.

2.2. Governing equations of joint elements

The governing equations of a joint element are derived from Equation (1). In most cases, it is assumed that an interface has negligible thickness. In this work, we will focus on the deformation response of the joint element developed by Goodman [10]. We disregard the inertial and damping contributions of interface elements to Equation (1). The virtual work, δW, or potential function, Π, for this element is obtained from Equation (1), as

$$\delta W = \int_A \delta u_j \left(\frac{\partial u_j}{\partial t^2}\rho + \sigma_{ij,i} + b_j\right) dA\,, \text{ and} \tag{3}$$

$$\Pi^{int} = \frac{1}{2}\int_A \varepsilon_{ij}\sigma_{ij}\,dA\,,$$

where δ means variation, $\boldsymbol{\varepsilon}$ is the small strain tensor, and the superscript *int* refers to internal energy or work.

By assuming infinitesimal thickness for the joint element, kinetic (stress) and kinematic (strain) terms associated with the thickness can be disregarded. Therefore, Equation (3) can be expressed in terms of two kinematic variables, which represent sliding and normal displacement along the joint (see Fig. 1), as follows:

$$\Pi^{int} = \frac{1}{2}\int_{-l/2}^{+l/2} k_n (v_{top} - v_{bottom})^2 d_x + k_s (u_{top} - u_{bottom})^2 d_x\,, \tag{4}$$

or

$$\Pi = \frac{1}{2}\int_A \mathbf{u}^T \mathbf{K}\mathbf{u}\,dA - \int_\Gamma \mathbf{u}^T \mathbf{F}\,d\Gamma\,, \tag{5}$$

where k_n and k_s are the normal and shear stiffness of the interface in dimensions of force/length, and $\mathbf{u}$, the displacement vector. $\mathbf{K}$, the stiffness matrix and $\mathbf{F}$, the internal force vector for the joint element, are derived from the minimization of potential energy as

$$\frac{\partial \Pi}{\partial \mathbf{u}} = \int_{+l/2}^{-l/2} \mathbf{K}\mathbf{u}\,dx - \int_\Gamma \mathbf{F}\,d\Gamma = 0\,, \tag{6}$$

where

$$K_{ij} = \frac{\partial \Pi}{\partial u_i \partial u_j} \text{ and } F_i = \frac{\partial \Pi}{\partial u_i}\,. \tag{7}$$

Equation (4) indicates that a joint element provides relaxed connectivity between two adjacent surfaces in contact (Fig. 1). It accomplishes this through force-relative displacement (of the surfaces) relationships. The degree of proportionality between force and displacement is captured through the normal, k_n, and tangential, k_s, stiffness coefficients.

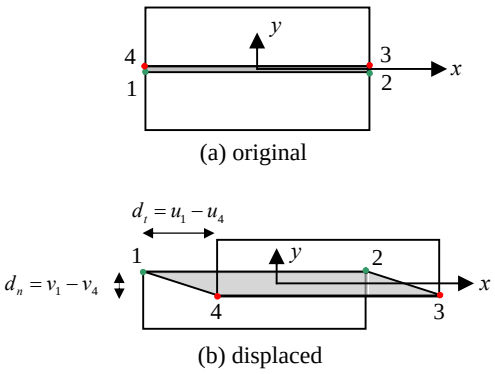

Fig. 1. Geometry and node topology of the Goodman FE interface element (1968) with four nodes and eight degrees of freedom: (a) in the original configuration nodes 1 and 4 share one position, while nodes 2 and 3 share another; (b) in the displaced configuration the nodes can move both normally and tangentially from each other.

2.3. Governing equations of discrete element techniques

In the mechanics of discrete assemblies of bodies, the governing equations of each discrete body follow from the linear momentum equation together with the traction boundary condition, which incorporates contact forces. Similar to continuum methods, discrete element techniques can be formulated based on the strong or weak form of Equation (1).

In a two-dimensional framework, for each discrete element, e, direct integration of the linear momentum equation over the area, A_e, leads to the following integral form

$$\int_{A_e} \frac{\partial u_j}{\partial t^2}\rho + \frac{\partial u_j}{\partial t}c + \sigma_{ij,i} + b_j dA = 0\,. \tag{8}$$

How the above expression is integrated depends on the spatial discretization technique used. Nevertheless, Equation (8) and its boundary condition reduce to the following system of equations at the nodes of the problem domain:

$$m_i\ddot{u}_i + c_i\dot{u}_i + F_i = 0\,, \tag{9}$$

where m_i represents the mass associated with the i^{th} degree of freedom, c_i is a damping term, and F_i includes the external loads, contact forces, damping forces and, if block deformability is considered, elastic deformation loads.

In energy-based discrete element methods, integration of the weak form of Equation (1) requires addition of a term representing the potential energy of the contact to the potential function obtained from Equation (1), i.e.,

$$\Pi_{system}^{total} = \sum_{e=1}^{e=n} \Pi_e^{total}\,, \tag{10}$$

where $\Pi_e^{total} = \int_{A_e} \Pi_e(\frac{\partial \ddot{u}_j}{\partial t^2}m, \frac{\partial \dot{u}_j}{\partial t^2}c, \sigma_{ij,i}, b_j) + \Pi_e^{contact}$.

The potential energy of the contact will be discussed in a subsection below. Minimizing this energy leads to a system of equations of the following form:

$$\mathbf{M\ddot{u}+C\dot{u}+Ku} = \mathbf{F}\,, \tag{11}$$

where $K_{ij} = \frac{\partial \Pi_{system}^{total}}{\partial u_i \partial u_j}$ and $F_i = \frac{\partial \Pi_{system}^{total}}{\partial u_i}$.

2.4. Governing equations of contact

Mathematically, contact is treated as a constraint on displacements at the interface of two objects. A normal contact condition prevents interpenetration of objects, while a tangential constraint enforces sticking/slipping.

Various numerical techniques have been developed to satisfy contact constraint conditions [20, 21]. The most widely-used methods are the Lagrange multiplier and the penalty approaches. The Lagrange approach strictly enforces impenetration and sticking, while the penalty method satisfies these constraints approximately.

The approximate enforcement of constraints by the penalty method is achieved through a proportionality law or penalty function that relates the degree of constraint violation to the size of the corrective measure. Any penetration violates the impenetrability constraint, and invokes contact forces that tend to return the surfaces to a state of compliance. Similarly, tangential penalty forces are developed as a result of relative tangential displacements at the contacting surfaces.

From the approximate enforcement of the normal impenetrability and tangential sticking constraints, the following potential energy terms arise:

$$\Pi^{contact} = \frac{1}{2}d_n\alpha_n d_n + \frac{1}{2}d_t\,\alpha_t d_t\,, \tag{12}$$

where α_n and α_t are the normal and tangential penalty coefficients, respectively, in dimensions of force per unit length.

Another technique for simulating contact is the soft (compliant) contact approach. This method does not constrain penetration displacements[2]. It assumes that

[2] In the hard contact approach no penetration is permitted. This definition becomes ambiguous in methods that satisfy the no-penetration constraint approximately. Therefore, we suggest defining a hard contact as a contact in which the penetration displacements are restricted to a specified tolerance.

springs exist at the contacts, and therefore infinitesimal penetration is permitted, and associated forces are calculated using the constitutive laws of the springs [22-24]. Assuming a linear constitutive spring relationship, $F = k\Delta l$, the potential function for each contact point becomes

$$\Pi^{contact} = \frac{1}{2}(k_n d_n^2 + k_t d_t^2), \tag{13}$$

where d_n and d_t are the normal and tangential displacements of a contact point on the boundary, measured with respect to the target surface with normal $\mathbf{n}$, and k_n and k_s are the normal and shear stiffnesses at the contact. Given that the penalty coefficients and the spring stiffnesses have the same dimensions, Equations (12) and (13) are equivalent.

To represent the energy contribution of contacts to a discrete system, Equation (13) can be arranged in the following vector-matrix form for all degrees of freedom related to all contacts:

$$\Pi^{contact} = \frac{1}{2}\mathbf{d}_n^T \boldsymbol{\alpha}_n \mathbf{d}_n + \frac{1}{2}\mathbf{d}_t^T \boldsymbol{\alpha}_t \mathbf{d}_t . \tag{14}$$

Equation (14) is the potential function term described earlier in Equation (10).

Minimization of the total potential energy with respect to displacements, gives the stiffness and force terms of Equation (11). By enforcing normal and tangential constraints, contact surfaces contribute force and stiffness terms, which can be expressed as

$$\left(F_n^{int}\right)_i^{contact} = \frac{\partial \prod^{contact}}{\partial u_i} \text{ or } \left(\mathbf{F}^{int}\right)_n^{contact} = \boldsymbol{\alpha}_n \mathbf{d}_n \frac{\partial \mathbf{d}_n}{\partial u}, \tag{15}$$

$$\left(K_n\right)_{ij}^{contact} = \frac{\partial \prod^{contact}}{\partial u_i \partial u_j} \text{ or}$$

$$\mathbf{K}_n^{contact} = \boldsymbol{\alpha}_n \left[\left(\frac{\partial \mathbf{d}_n}{\partial \mathbf{u}} \right)^T \frac{\partial \mathbf{d}_n}{\partial \mathbf{u}} + \mathbf{d}_n \frac{\partial}{\partial \mathbf{u}} \left(\frac{\partial \mathbf{d}_n}{\partial \mathbf{u}} \right) \right],$$

$$\left(F_t^{int}\right)_i^{contact} = \frac{\partial \prod^{contact}}{\partial u_i} \text{ or } \left(\mathbf{F}^{int}\right)_t^{contact} = \boldsymbol{\alpha}_t \mathbf{d}_t \frac{\partial \mathbf{d}_t}{\partial \mathbf{u}}, \tag{16}$$

$$\left(K_t\right)_{ij}^{contact} = \frac{\partial \prod^{contact}}{\partial u_i \partial u_j} \text{ or}$$

$$\mathbf{K}_t^{contact} = \boldsymbol{\alpha}_t \left[\left(\frac{\partial \mathbf{d}_t}{\partial \mathbf{u}} \right)^T \frac{\partial \mathbf{d}_t}{\partial \mathbf{u}} + \mathbf{d}_t \frac{\partial}{\partial \mathbf{u}} \left(\frac{\partial \mathbf{d}_t}{\partial \mathbf{u}} \right) \right].$$

By disregarding the second term of the stiffness matrices, the combined forms of Equations (15) and (16) become

$$\mathbf{F}^{int} = \begin{bmatrix} \boldsymbol{\alpha}_t & \mathbf{0} \\ 0 & \boldsymbol{\alpha}_n \end{bmatrix} \mathbf{d} \frac{\partial \mathbf{d}}{\partial \mathbf{u}} \text{ , and} \tag{17}$$

$$\mathbf{K} = \left(\frac{\partial \mathbf{d}}{\partial \mathbf{u}} \right)^T \begin{bmatrix} \boldsymbol{\alpha}_t & \mathbf{0} \\ 0 & \boldsymbol{\alpha}_n \end{bmatrix} \frac{\partial \mathbf{d}}{\partial \mathbf{u}},$$

and the potential function is

$$\Pi^{contact}(\mathbf{u}) = \frac{1}{2}\mathbf{u}^T \mathbf{K}\mathbf{u} - \mathbf{F}^T \mathbf{u}, \tag{18}$$

where $\mathbf{u}$ is the displacement vector, $\mathbf{K}$, the $n \times n$ linear symmetric contact stiffness matrix, $\mathbf{F}$, the applied load vector and *n,* the number of degrees of freedom associated with the nodes that are in contact.

2.5. Comparison of governing equations

The previous sub-sections showed that the linear momentum equation, expressed by Equation (1), is the governing equation for both combined continuum-interface techniques and discrete element techniques. The linear momentum equation leads to a spatially-discretized system of equations of the form $\mathbf{M}\ddot{\mathbf{u}}+\mathbf{C}\dot{\mathbf{u}}+\mathbf{K}\mathbf{u} = \mathbf{F}$ or $m_i\ddot{u}_i + c_i\dot{u}_i + F_i = 0$. These equations are nearly identical with the only difference being that, in the latter, the governing equations are decoupled for each degree of freedom *i*.

Both contact enforcement and the joint element define normal (impenetrability) and tangential constitutive responses at the interface between two objects. Approximate enforcement of the contact impenetrability condition and tangential constitutive law results in force and stiffness terms expressed by Equations (4-7). Similarly, a joint element – an entity that represents a continuum with negligible thickness in one direction – enforces the normal and tangential constitutive responses at the interface as expressed by Equations (17-18).

Numerical evaluation of the stiffness and force terms arising from the contact enforcement approach and joint element will be discussed in Section 4. However, comparison of Equations (4-7) to Equations (17-18) shows that the stiffness and force expressions represent identical physical responses at an interface. These terms contribute to the global stiffness and force components for the system of discrete objects. It is worthy to note that the spring-type stiffness k and the penalty parameter α have similar dimensions. They both represent constants of proportionality in the laws that relate forces to normal and relative tangential displacements.

In addition to conservation of linear momentum, the governing equations of discontinuous media, require conservation of angular momentum. In continuum-based methods, angular momentum is implicitly satisfied through stress tensor symmetry at every point in a body. For methods, such as discrete element techniques, in which the forces acting on a body are resolved only at the body's centroid, angular momentum needs to be

explicitly represented in the system of equations. This is required to satisfy the laws of vector translation. As a result, the explicit representation of angular momentum in the equations of discrete techniques should not be viewed as an advantage over continuum-based methods.

3. KINEMATICS

It has been shown in this paper that both contact enforcement and joint elements contribute to the force and stiffness terms of a discontinuous problem. However, the manner in which these terms are evaluated differs. Terms for joint elements are generally evaluated based on the same standard space-discretization methods used in continuum methods such as the FEM. Since contacts change with time, evaluation of these terms depends on contact kinematics at the moment of evaluation.

3.1. Kinematics of the joint element

The following three assumptions are intrinsic to the kinematics of the Goodman joint element:

(i) The joint element is a reduced form of a quadrilateral solid element with negligible thickness,

(ii) The two sides of the joint element have equal length, and

(iii) The joint element defines an edge-to-edge contact in which connectivity (joint node pairings) does not change with time.

3.2. Kinematics of contact

From a physical point of view, there are three kinematically feasible modes of contact between two objects (shown in Fig. 2). Different contact resolution techniques have been developed for evaluating the force and stiffness terms of Equation (17). Some techniques consider all three possible modes of contact depicted in Fig. 2, while others resolve mode (c) into two node-to-edge contacts. A technique proposed by Munjiza can resolve contact terms without considering contact modes by evaluating areas of overlap instead [25].

In addition to contact kinematics, the contact resolution technique adopted in a discrete element technique depends on the shape (e.g., circles or polygons) it assumes for discrete bodies and the spatial discretization method it uses. For example, the Bonded Particle Model [24] assumes discrete objects to be circular disks or spheres. Therefore, contact resolution in the Bonded Particle Model becomes greatly simplified, and contact penetration displacement can be evaluated simply through the relative position of centres of adjacent objects. In techniques that discretize arbitrarily-shaped blocks into elements or grid points, penetration and relative sliding displacements can be evaluated for block vertices or mesh nodes that are in contact.

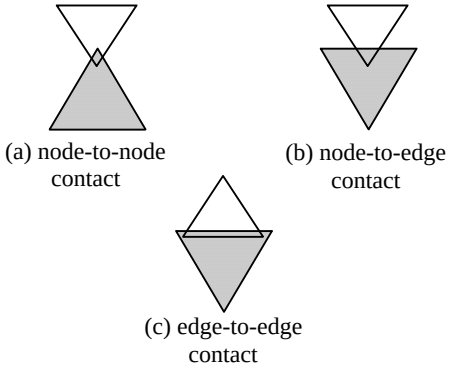

Fig. 2. Three possible type of physical contact in a 2D framework.

3.3. Comparison of kinematics of contact and joint element

The Goodman joint element models the discontinuous displacement response that arises at an edge-to-edge contact or interface. The normal and tangential displacements at the interface are measured in terms of the relative displacements of the nodal pairs of the edges (see Fig. 1). The Goodman joint assumes that, even though edges displace relative to each other, edge pairings remain constant.

Unlike joint elements, contacts in discrete element techniques are not restricted to edge-to-edge mode only (see Fig. 2). Contact pairings can also change throughout the solution process. Therefore, discrete element techniques require algorithms for

1. Updating the positions of discrete objects, and
2. Determining newly formed contacts or detached contacts.

4. EXAMPLE OF EDGE-TO-EDGE CONTACT

To demonstrate the similarities between mathematical terms arising from joint element and contact enforcement, the simple problem shown in Fig. 3, which represents an edge-to-edge contact, is solved using two different approaches: (i) two finite elements attached by a joint element, and (ii) two discrete elements with an edge-to-edge contact.

4.1. Stiffness and force terms of a joint element

The joint element applied in this paper is a four-noded, one-dimensional finite element designed to simulate shear and normal displacements of interfaces. Since the two sides of the joint element have equal length, the finite element shape functions for nodes 1 and 4, and nodes 2 and 3 (see Fig. 3) will be similar. Therefore, the displacement field can be interpolated as

$$u = N_1(u_1 - u_4) + N_2(u_2 - u_3)\,, \tag{19}$$

$$v = N_1(v_1 - v_4) + N_2(v_2 - v_3)\,,$$

or in vector-matrix form

$$\mathbf{u}=\mathbf{B}\bar{\mathbf{u}}=\begin{bmatrix} N_1 & 0 & N_2 & 0 & -N_2 & 0 & -N_1 & 0 \\ 0 & N_1 & 0 & N_2 & 0 & -N_2 & 0 & -N_1 \end{bmatrix}\bar{\mathbf{u}}, \tag{20}$$

where

$$\bar{\mathbf{u}} = \begin{bmatrix} u_1 & v_1 & u_2 & v_2 & u_3 & v_3 & u_4 & v_4 \end{bmatrix}.$$

Matrix $\mathbf{B}$ relates the displacement field $\mathbf{u}$ to the nodal degrees of freedom, $\bar{\mathbf{u}}$.

The stiffness and force terms can be determined by substituting Equation (20) into Equation (6), and integrating over the length, l, of the joint to obtain

$$\mathbf{K} = \int_{-l/2}^{+l/2} \mathbf{B}^{\mathrm{T}}\mathbf{D}\mathbf{B}\,dx \;\text{ with }\; \mathbf{D} = \begin{bmatrix} k_s & 0 \\ 0 & k_n \end{bmatrix}, \tag{21}$$

$$\mathbf{K} = \frac{l}{6}\begin{bmatrix} 2k_s & 0 & 1k_s & 0 & -1k_s & 0 & -2k_s & 0 \\ 0 & 2k_n & 0 & 1k_n & 0 & -1k_n & 0 & -2k_n \\ 1k_s & 0 & 2k_s & 0 & -2k_s & 0 & -1k_s & 0 \\ 0 & 1k_n & 0 & 2k_n & 0 & -2k_n & 0 & -1k_n \\ -1k_s & 0 & -2k_s & 0 & 2k_s & 0 & 1k_s & 0 \\ 0 & -1k_n & 0 & -2k_n & 0 & 2k_n & 0 & 1k_n \\ -2k_s & 0 & -1k_s & 0 & 1k_s & 0 & 2k_s & 0 \\ 0 & -2k_n & 0 & -1k_n & 0 & 1k_n & 0 & 2k_n \end{bmatrix}$$

and

$$\mathbf{F}=\int_{-l/2}^{+l/2} \mathbf{B}^{\mathrm{T}}\mathbf{D}\bar{\mathbf{u}}\,dx\,. \tag{22}$$

4.2. Stiffness and force terms for discrete objects with edge-to-edge contact

To evaluate the contact stiffness matrix and force vector of contact as expressed by Equation (17) the term $\partial\mathbf{d}/\partial\mathbf{u}$ must be determined. We do so by applying a commonly-used technique that computes the distances over which a point on the object, $\mathbf{x}_s$, penetrates into and slides over the smooth and continuous boundary surface of the target object $\partial\Omega$.

Edge-to-edge contact is treated as two node-to-edge contacts. Normal penetration, d_n, and tangential displacement, d_t can be expressed as

$$d_n = \begin{bmatrix}\mathbf{n} & -\mathbf{n}\end{bmatrix}\begin{Bmatrix}\mathbf{x}_s \\ \mathbf{x}_{\partial\Omega}\end{Bmatrix},\; d_t = \begin{bmatrix}\mathbf{t} & -\mathbf{t}\end{bmatrix}\begin{Bmatrix}\mathbf{x}_s \\ \mathbf{x}_{\partial\Omega}\end{Bmatrix}, \tag{23}$$

where $\mathbf{x}$, the current position vector of a node, is given by

$$\mathbf{x}=\mathbf{X}+\mathbf{u}\,, \tag{24}$$

$\mathbf{n}$ is the normal to the contact surface, $\mathbf{t}$ is the tangent to the contact surface, $\mathbf{X}$ is the original position vector of the node, and $\mathbf{u}$ is the node displacement vector.

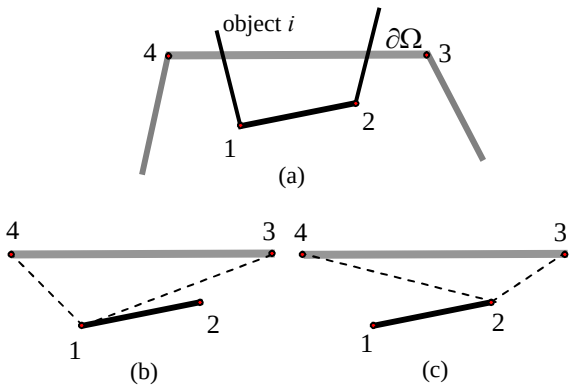

Fig. 3. Edge-to-edge contact, (a) penetration of the edge 1-2 belonging to object *i* into object *j*, (b) penetration of node 1 to the edge 3-4, (c) penetration of node 2 into the edge 2-3.

The normal penetration distance for point 1 belonging to block i with respect to edge 3-4 belonging to block j (see Fig. 3) can be obtained as

$$d_n = \begin{vmatrix} 1 & 1 & 1 \\ X_1+u_1 & X_3+u_3 & X_4+u_4 \\ Y_1+v_1 & Y_3+v_3 & Y_4+v_4 \end{vmatrix}, \tag{25}$$

or

$$\begin{aligned} d_{n1} = S_{01} &+ \begin{bmatrix} Y_3-Y_4 & X_4-X_3 \end{bmatrix}\begin{bmatrix} u_1 \\ v_1 \end{bmatrix} \\ &+ \begin{bmatrix} Y_4-Y_1 & X_1-X_4 \end{bmatrix}\begin{bmatrix} u_3 \\ v_3 \end{bmatrix}\,, \\ &+ \begin{bmatrix} Y_1-Y_3 & X_3-X_1 \end{bmatrix}\begin{bmatrix} u_4 \\ v_4 \end{bmatrix} \end{aligned} \tag{26}$$

where

$$S_{01} = \begin{vmatrix} 1 & 1 & 1 \\ X_1 & X_3 & X_4 \\ Y_1 & Y_3 & Y_4 \end{vmatrix}. \tag{27}$$

A similar derivation for node 2 leads to

$$\begin{aligned} d_{n2} = S_{02} &+ \begin{bmatrix} Y_3-Y_4 & X_4-X_3 \end{bmatrix}\begin{bmatrix} u_2 \\ v_2 \end{bmatrix} \\ &+ \begin{bmatrix} Y_4-Y_2 & X_2-X_4 \end{bmatrix}\begin{bmatrix} u_3 \\ v_3 \end{bmatrix} \\ &+ \begin{bmatrix} Y_2-Y_4 & X_3-X_2 \end{bmatrix}\begin{bmatrix} u_4 \\ v_4 \end{bmatrix}. \end{aligned} \tag{28}$$

At any time *t*, the normal penetration distance is evaluated only using the current position of the contacting nodes of the two objects. This however is not the case with tangential displacements. Their evaluation depends on the displacement history of the nodes. In other words, the tangential displacement for each penetrating node is measured incrementally with respect

to a reference point on the target object. This reference point is the point on the target object surface at which the penetrating node first makes contact (see Fig. 4). The total tangential displacement for a node is then the sum of incremental displacements it has experienced through time.

The expression for d_t is derived assuming point 4 to be the target (reference) point for point 1, and point 3 to be the target for point 2. The expression for tangential displacement is then

$$d_{t1} = \begin{bmatrix} X_1 + u_1 - (X_3 + u_3) & Y_1 + v_1 - (Y_3 + v_3) \end{bmatrix} . \mathbf{t} \ . \tag{29}$$

A similar procedure is used to evaluate the normal penetration and tangential displacement of nodes 3 and 4 with respect to surface 1-2, with the target and penetrator objects now switched around.

To numerically solve the system of equations for a problem, d_n and d_t must be expressed in terms of the unknowns associated with the degrees of freedom of the system.

If the blocks were to be discretized into an FEM mesh or FDM grid, then d_n and d_t would be directly expressed in terms of the unknown nodal displacements. Therefore, for the contact shown in Fig. 3, the displacement field over the contacting edges can be expressed in terms of the following nodal degrees of freedom:

$$\bar{\mathbf{U}} = \begin{bmatrix} u_1 & v_1 & u_2 & v_2 & u_3 & v_3 & u_4 & v_4 \end{bmatrix} . \tag{30}$$

Equation (17) for the contact results in an 8×8 stiffness matrix, and an 8×1 force vector.

In order to check the equivalence of the joint element formulation to contact enforcement, the variation of d_n and d_t along the penetration edge is considered.

Using Equations (26) and (29), the normal penetration, d_n^x, and tangential displacement, d_t^x, of a point $\mathbf{x}$ on edge 1-2 of object i can be expressed as

$$\begin{aligned} d_n^x = & \frac{1}{l_{23}} (S_{0x} + (X_4 - X_3) v_x + (X - X_4) v_3 \\ & + (X_3 - X) v_4 + (Y_3 - Y_4) u_x + (Y_4 - Y) u_3 + (Y_3 - Y) u_4), \end{aligned} \tag{31}$$

and

$$d_t^x = \begin{bmatrix} (X+u)^{penetrator} - (X+u)^{target} & (Y+v)^{penetrator} - (Y+v)^{target} \end{bmatrix} . \mathbf{t}^{target} \ . \tag{32}$$

In order to compare terms arising from the contact formulation with those from interface elements, we enforce the kinematic assumptions of the joint element and analytically resolve the contact terms. Although this approach is not used in numerical implementations, the conclusions drawn from it are general.

Without any loss of generality, an edge-to-edge contact involving two objects with different edge lengths can be discretized into a contact of two objects with equal edge size. In that case the locations of nodes 3 and 4 are placed at the points where nodes 1 and 2 first contact the edge of object j. It can also be assumed that the normal to the contact surface is parallel to the global Y coordinate axis.

To compare the stiffness and force terms of the joint element and contact enforcement, further assumptions need to be made. First, it must be assumed that edges 1-2 and 3-4 are parallel at the instant contact occurs. This is compatible with the kinematics of a joint element. Although the assumption is physically meaningful, it may not be satisfied numerically in the approximate enforcement of impenetrability.

Equations (31) and (32) then reduce to

$$d_n^x = \frac{1}{l_{23}} (l_{34} v_x + (X - X_4) v_3 + (X_3 - X) v_4) , \tag{33}$$

and

$$d_t^x = N_1 (v_1 - v_4) + N_2 (v_2 - v_3) , \tag{34}$$

where $v_x = N_1 v_1 + N_2 v_2$.

The position vector x can be expressed in terms of nodal positions along the contacting edges (Fig. 4) as

$$x - x_4 = \zeta \ \text{ and } \ x_3 - x = l - \zeta , \tag{35}$$

where $0 \le \zeta \le l$.

Equations (33) and (34) become

$$\begin{aligned} d_n &= (N_1 v_1 + N_2 v_2) - \frac{1}{l_{34}} (\zeta v_3 + (l - \zeta) v_4) \\ &= (N_1 v_1 + N_2 v_2) - (N_3 v_3 + N_4 v_4), \end{aligned} \tag{36}$$

and

$$d_t = (N_1 u_1 + N_2 u_2) - (N_3 u_3 + N_4 u_4) . \tag{37}$$

Finally, by assuming that the contacting lengths are equal (i.e. $l_{12} = l_{34}$), then $N_1 = N_3$ and $N_2 = N_4$, and Equations (36) and (37) can be rearranged in the form

$$\mathbf{d} = \begin{bmatrix} d_t \\ d_n \end{bmatrix} = \begin{bmatrix} N_1 & 0 & N_2 & 0 & -N_4 & 0 & -N_2 & 0 \\ 0 & N_1 & 0 & N_2 & 0 & -N_3 & 0 & -N_1 \end{bmatrix} \bar{\mathbf{U}} = \mathbf{B} \bar{\mathbf{U}} . \tag{38}$$

Substituting (38) into the stiffness matrix of Equation (17) leads to

$$\mathbf{K} = \int_l \mathbf{B}^{\mathbf{T}} \begin{bmatrix} \alpha_t & 0 \\ 0 & \alpha_n \end{bmatrix} \mathbf{B} dx , \tag{41}$$

and

$$\mathbf{K} = \int_{-l/2}^{+l/2} \mathbf{A}\,dx. \text{, with} \tag{42}$$

$$\mathbf{A} = \begin{bmatrix} N_1^2\alpha_t & 0 & N_1N_2\alpha_t & 0 & -N_1N_2\alpha_t & 0 & -N_1^2\alpha_t & 0 \\ 0 & N_1^2\alpha_n & 0 & N_1N_2\alpha_n & 0 & -N_1N_2\alpha_n & 0 & -N_1^2\alpha_n \\ N_1N_2\alpha_t & 0 & N_2^2\alpha_t & 0 & -N_2^2\alpha_t & 0 & -N_1N_2\alpha_t & 0 \\ 0 & N_1N_2\alpha_n & 0 & N_2^2\alpha_n & 0 & -N_2^2\alpha_n & 0 & -N_1N_2\alpha_n \\ -N_1N_2\alpha_t & 0 & -N_2^2\alpha_t & 0 & N_1^2\alpha_t & 0 & N_1N_2\alpha_t & 0 \\ 0 & -N_1N_2\alpha_n & 0 & -N_2^2\alpha_n & 0 & N_1^2\alpha_n & 0 & N_1N_2\alpha_n \\ -N_1^2\alpha_t & 0 & -N_1N_2\alpha_t & 0 & N_1N_2\alpha_t & 0 & N_2^2\alpha_t & 0 \\ 0 & -N_1^2\alpha_n & 0 & -N_1N_2\alpha_n & 0 & N_1N_2\alpha_n & 0 & N_2^2\alpha_n \end{bmatrix}.$$

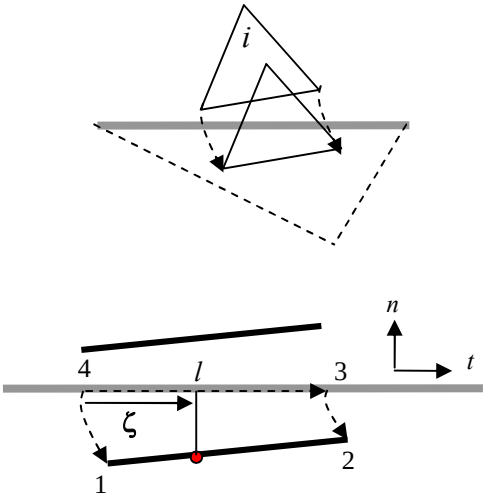

Fig. 4. Distributed force approach to an edge-to-edge contact of two objects.

Assuming that displacements over a contact length vary linearly according to the forms $u = N_1u_1 + N_2u_2$ with $N_1 = (1/l)x$, and $N_2 = (1/l)(l-x)$, integration of Equation (42) results in

$$\mathbf{K} = \frac{l}{6}\begin{bmatrix} 2\alpha_t & 0 & 1\alpha_t & 0 & -1\alpha_t & 0 & -2\alpha_t & 0 \\ 0 & 2\alpha_n & 0 & 1\alpha_n & 0 & -1\alpha_n & 0 & -2\alpha_n \\ 1\alpha_t & 0 & 2\alpha_t & 0 & -2\alpha_t & 0 & -1\alpha_t & 0 \\ 0 & 1\alpha_n & 0 & 2\alpha_n & 0 & -2\alpha_n & 0 & -1\alpha_n \\ -1\alpha_t & 0 & -2\alpha_t & 0 & 2\alpha_t & 0 & 1\alpha_t & 0 \\ 0 & -1\alpha_n & 0 & -2\alpha_n & 0 & 2\alpha_n & 0 & 1\alpha_n \\ -2\alpha_t & 0 & -1\alpha_t & 0 & 1\alpha_t & 0 & 2\alpha_t & 0 \\ 0 & -2\alpha_n & 0 & -1\alpha_n & 0 & 1\alpha_n & 0 & 2\alpha_n \end{bmatrix}, \tag{43}$$

and

$$\mathbf{F}=\mathbf{K}\bar{\mathbf{u}} \text{ or } \mathbf{F}=\mathbf{B}\begin{bmatrix} \alpha_t & 0 \\ 0 & \alpha_n \end{bmatrix}\bar{\mathbf{u}}\,.$$

4.3 Comparison of stiffness and force terms

In Section 2 it was concluded that contact enforcement and the joint element both result in stiffness and force terms. It was also discussed that the penalty parameter and joint stiffness have the same dimensions and represent identical physical behaviors. Comparison of Equations (21) and (43) shows that under the assumptions discussed in the current section, numerical evaluation of the stiffness matrix of an edge-to-edge contact is identical to that arising from an interface element. Similarly, it can be deduced that the force terms are identical.

5. CONCLUSIONS

This paper compares the combined continuum-interface and discrete element techniques in analysis of jointed rock masses. It examines the

1. Governing equations and assumptions of continuum and discontinuum mechanics,
2. Formulation of joint/interface elements,
3. Mathematics and kinematics of contact, and interface elements.

The governing equations of both continuum and discontinuous mechanics are based on the conservation of linear and angular momentum. Both combined continuum-interface methods and discrete element techniques explicitly simulate discontinuous surfaces, using special joint elements and contact considerations, respectively. Both approaches can accurately capture the discontinuous changes in the deformation, stress, and strain fields of discrete objects.

This paper shows that the joint element and enforcement of contact constraints lead to stiffness and force terms at an interface. By enforcing kinematic assumptions of joint element on the case of an edge-to edge contact, we showed that both techniques lead to identical expressions for stiffness and force.

The arguments in the paper emphasize that, at a specific instance in time, if an assembly of discrete objects with edge-to-edge contacts were to be replaced by a combined continuum-interface model, the resulting algebraic equations would be identical. (Clearly this is true only if both techniques adopt similar assumptions on the deformability of objects.)

Joint elements readily model the reduced normal and tangential resistances of contact surfaces. From a kinematic point of view, their most appropriate use is in the modeling of edge-to-edge contact. Because of the defined joint topology, they are also restricted to problems in which pairing between two contacting objects does not change. In combined continuum-joint problems, once interconnectivity between solid and joint elements is established upon meshing, it remains unchanged throughout the solution process, despite the displacements that occur.

In contrast, when contacts are used (by discrete element techniques) to represent physical interfaces, their

kinematics are completely unrestricted; old contacts can be broken and new ones established, and contact modes can change. As a result, discrete element techniques must check for released contacts and newly formed ones throughout the solution process.

Due to the above-described characteristics, the choice between combined continuum-interface methods and discrete element techniques depends on the configuration of an assembly of discrete blocks, and how it evolves over time. Continuum-based methods that use joint elements are accurate provided changes in edge-to-edge contacts are insignificant throughout the solution [26, 27]. These methods can accommodate large displacements, rotations, or strains of discrete objects, so long as these mechanisms do not change contacting node couples. Discrete element methods, on the other hand, can accommodate problems in which block connectivity changes extensively.

It is hoped that this discussion clarifies some of the misconceptions in the geomechanics community of what the differences are between the numerical methods. It suggests that the term *discrete element technique* should refer to all numerical models that are developed with the primary purpose of modeling assemblies of blocks or particles. Aspects such as large deformation, freedom in contact modes, and change in contacting couples are three aspects deemed inherent to all discrete element models. However, they are also shared by some continuum-based implementations [28]. Therefore, what differentiates the deformable-block discrete element techniques from continuum methods, which accommodate these assumptions, is merely the presence of algorithms that facilitate generation and analysis of large scale discrete problems.

ACKNOWLEDGEMENTS

The support of the National Science and Engineering Research Council (NSERC), through a Discovery Grant to J.H. Curran and an Industrial Research and Development Fellowship to Azadeh Riahi, is greatly acknowledged.

REFERENCES

[1] Cundall, P.A. 1971. A computer model for simulating progressive, large scale movements in blocky rock systems. In *Proceedings of the International Symposium Rock Fracture*. Nancy, France. 2-8.

[2] Cundall, P.A., R.D. Hart. 1992. Numerical modeling of discontinua. *Engineering Computations*. 9(2), 101-113.

[3] Cundall, P.A., O.D.L. Strack. 1979. A discrete model for granular assemblies. *Geotechnique*. 29(1), 47-65.

[4] Potyondy, D., P.A. Cundall. 2004. A bonded particle model for rock. *International Journal for Rock Mechanics and Mining Science*. 41, 1329-1364.

[5] Shi, G. 1988. *Discontinuous deformation analysis: A new numerical model for the statics and dynamics of locked systems*. Ph.D. thesis, University of California, Berkeley.

[6] Belytschko, T., W.K Liu., B. Moran. 2000. *Nonlinear finite elements for continua and structures*. New York: John Wiley.

[7] Zienkiewicz, O.C., R.L. Taylor. 2005. *The finite element method*. 6th edition, New York: Elsevier.

[8] Griffiths, D.V., S. Smith. 2006. *Numerical methods for engineers*. 2nd edition, CRS Press.

[9] Banerjee, P.K. 1994. *The boundary element methods in Engineering*. McGraw-Hill College.

[10] Goodman, R.E., R.L. Taylor, T.L. Brekke. 1968. A model for mechanics of jointed rock. *Journal of the Soil Mechanics and Foundation Division*. 94, 637-659.

[11] Zienkiewicz, O.C., B. Best, C. Dullage, K.C. Stagg. 1970. Analysis of nonlinear problems in rock mechanics with particular reference to jointed rock systems. In *Proceedings of the 2nd International Conference of the Society of Rock Mechanics*. Belgrade, 8-14.

[12] Gaboussi, J., E.L. Wilson, J. Isenberg. 1974. Finite elements for rock joints and interfaces. *Journal of the Soil Mechanics and Foundation Division*. A.S.C.E., 99, 833-848.

[13] Wilson, E.L. 1977. Finite elements for foundations, joints and fluids. *Finite Elements in Geomechanics.* John Wiley, Chapter 10.

[14] Pande, G.N., K.G. Sharma. 1979. On Joint/interface elements and associated problems of numerical ill-conditioning. *International Journal of Numerical Methods in Geomechanics*. 2, 293-300.

[15] Tzamtzis, A. 2003. Finite element modeling of cracks and joints in discontinuous structural systems, In *the 16th ASCE Engineering Mechanics Conference*. Seattle.

[16] Dyszlewicz, J. 2004 *Micropolar theory of elasticity*. New York: Springer.

[17] Cosserat, E., F. Cosserat. 1909. *Théorie des corps déformables*. Paris: Hermann.

[18] Mühlhaus, H.B. 1993. Continuum models for layered and blocky materials. In *Comprehensive rock mechanics*. Pergamon Press, 209-230.

[19] Mühlhaus, H.B. 1995. A relative gradient model for laminated material. In *Continuum models for materials with microstructure*. Toronto: Wiley, Chapter 13.

[20] Mohammadi, S. 2003. *Discontinuum mechanics, using finite and discrete Elements*. Southhampton: WIT Press.

[21] Wriggers, P. 2002. *Computational contact mechanics*. N.J.: John Wiley & Sons.

[22] Itasca Inc. 2003. *3DEC, Three-dimensional distinct universal code*. Version 4. Minneapolis, Minnesota, USA.

[23] Itasca Inc. 2004. UDEC, *Two-dimensional distinct universal code*. Version 4. Minneapolis, Minnesota, USA.

[24] Itasca Inc. 2001. *PFC, Particle flow code in two dimensions*. Version 2. Minneapolis, Minnesota, USA.

[25] Munjiza A. 2004. *The combined finite-discrete element method*, Wiley.

[26] Hammah, R.E., T.E. Yacoub, B. Corkum, J.H. Curran. 2008. The practical modeling of discontinuous rock masses with finite element analysis. In *Proceedings of the 42nd U.S. Rock Mechanics Symposium – 2nd U.S.-Canada Rock Mechanics Symposium*. San Francisco, US.

[27] Hammah, R.E., T.E. Yacoub, B. Corkum, F. Wibowo, J.H. Curran. 2007. Analysis of blocky rock slopes with finite element shear strength reduction analysis, In *Proceedings of the 1st Canada-U.S. Rock Mechanics Symposium*. Vancouver, Canada.

[28] Livermore Software Technology Corp. 2006, *LS-DYNA Theory Manual*. Livermore, California.